Zoosyst. Evol. 101 (4) 2025, 2357–2367 | DOI 10.3897/zse.101.170695

PENSOFT

MUSEUM FÜR NATURKUNDE BERLIN

Taxonomy and phylogeny of *Myxobolus branchiostegi* sp. nov. (Myxozoa, Myxosporea) infecting the gallbladder of *Branchiostegus argentatus* Cuvier, 1830 from the East China Sea

Yalin Xiong[1], Yuanjun Zhao[1], Xue Chen[1], Mao Wang[1], Jianjun Peng[2], Xiaojuan Cui[2], Chengzhong Yang[1]

1 *Animal Biology Key Laboratory of Chongqing Education Commission of China, Chongqing Key Laboratory of Conservation and Utilization of Freshwater Fishes, College of Life Sciences, Chongqing Normal University, Chongqing 401331, China*

2 *School of Life and Health Sciences, Hunan University of Science and Technology, Xiangtan 411201, China*

https://zoobank.org/EB8ADAF4-C9B6-494C-943A-1717E9581529

Corresponding author: Chengzhong Yang (drczyang@126.com)

Academic editor: Pavel Stoev ♦ **Received** 1 September 2025 ♦ **Accepted** 14 November 2025 ♦ **Published** 27 November 2025

Abstract

Myxobolus branchiostegi **sp. nov.** was detected in the gallbladder of six out of 28 specimens (21.4%) of *Branchiostegus argentatus* Cuvier, 1830 from the East China Sea. This is the first record of a *Myxobolus* species infecting this host. Mature myxospores of the new species were oval in valvular view, measuring 9.21 ± 0.52 µm (8.3–9.8 µm) in length and 7.40 ± 0.60 µm (6.2–8.0 µm) in width. Two equal, pyriform polar capsules measured 4.40 ± 0.34 µm (3.7–4.8 µm) in length and 2.58 ± 0.17 µm (2.3–2.9 µm) in width, each possessing polar tubules with 4–6 turns. Phylogenetic analysis, based on small subunit ribosomal RNA gene (SSU rDNA) sequences placed the new species within the family Myxobolidae, as a sister to *Myxobolus iwagiensis* Kawano et al., 2025. Further analysis suggested a possible trend that the clustering of Myxobolidae species may be influenced by the taxonomic affinity of their fish hosts, with closely-related parasites tending to infect hosts within the same order. Host aquatic habitat (marine, brackish-water or freshwater) and species geographic distribution may also contribute to the observed clustering patterns.

Key Words

Branchiostegus argentatus, *Myxobolus branchiostegi* sp. nov., phylogeny, SSU rDNA, taxonomy

Introduction

Myxozoans are highly diverse obligate endoparasites belonging to the phylum Cnidaria (Okamura et al. 2015; Yang et al. 2017; Zhang et al. 2019; Tilley et al. 2024). These organisms primarily infect fish inhabiting freshwater, brackish-water and marine environments; however, a few have also been documented infecting bryozoans, amphibians, reptiles, birds and mammals (Okamura et al. 2015; Székely et al. 2015; Liu et al. 2019; Shi et al. 2022). Some myxozoan species exhibit high pathogenicity in some commercially valuable fish, such as salmon and trout (e.g. *Oncorhynchus mykiss*, *Oncorhynchus kisutch*, *Salmo trutta*, *Oncorhynchus nerka* and *Oncorhynchus tshawytscha* etc.), causing growth retardation and, in some cases, mass mortality (Alexander et al. 2014; Carraro et al. 2016; Saha and Bandyopadhyay 2018; Guo et al. 2021). Particularly, some myxozoans have been reported to pose a risk of food-borne illness, potentially causing symptoms such as diarrhoea or vomiting in humans (Boreham et al. 1998; Harada et al. 2012; Kim et al. 2018).

Myxobolus Bütschli, 1882 is the largest genus within the Myxozoa, encompassing a high diversity of species, with over 1000 species to date, accounting for nearly one-third of all described myxozoans (Okamura et al. 2018; Eiras et al. 2021; Vieira et al. 2024; de Sena et al. 2025). *Myxobolus* can parasitise various sites, including the skin, intestines, spleen, ovaries, liver, eyes, gallbladder,

Copyright *Xiong, Y. et al*. This is an open access article distributed under the terms of the Creative Commons Attribution License (CC BY 4.0), which permits unrestricted use, distribution, and reproduction in any medium, provided the original author and source are credited.

gills and others (Eiras et al. 2005; Eiras et al. 2014; Eiras et al. 2021). The simplified morphology of myxospores results from extensive evolutionary reduction associated with parasitism (Lom and Dyková 2006). This extreme morphological simplification and high degree of convergence significantly limit the availability of reliable taxonomic characters (Fiala et al. 2015). Additionally, many researchers have realised that the spore morphology of some myxosporeans are plastic (Gao et al. 2020; Yang et al. 2023). Therefore, relying solely on morphological characteristics for the diagnosis of *Myxobolus* species may not guarantee the accuracy of the identification (Zhang et al. 2019; Gao et al. 2020). Currently, it is highly recommended to employ a combination of morphology, SSU rDNA sequences and information of host species, infection site (tissue tropism) and geographic locality for the identification of myxozoans (Zhao et al. 2013; Fiala et al. 2015; Liu et al. 2016; Yang et al. 2023).

In a recent investigation of myxozoan diversity in fish from the East China Sea, a novel species of *Myxobolus* parasitising the gallbladder of *Branchiostegus argentatus* Cuvier, 1830 was found. In the present study, an integrative taxonomic approach incorporating morphological, molecular, host and geographic locality data was used to describe the new species.

Materials and methods

Sample collection and morphological analyses

The fish hosts (n = 28) were captured by a commercial fishing boat from the coastal waters of Xiamen, East China Sea, China, on 23 July 2017 (sampling sites shown in Fig. 1) and subsequently transported to the laboratory. The total lengths of these fish ranged from 19 to 22 cm.

Figure 1. Map showing sampling locality for hosts of *Myxobolus branchiostegi* sp. nov.

Fish were identified, based on morphological characteristics and DNA barcoding of the mitochondrial cytochrome c oxidase subunit I (*COI*) gene, confirming all 28 specimens as *B. argentatus*. Multiple fish organs (skin, fins, gills, muscles, hepatopancreas, intestine, spleen, heart, gallbladder and urinary bladder) and body fluids (bile, blood and urine) were examined for myxozoan infections. Isolated parasite spores were collected for morphological and molecular analyses. Species identification and specimen treatment were carried out following previously described methods (Zhao et al. 2001). Myxospores were examined fresh and measured using a Leica DM6000B microscope at 1,000× magnification. Measurements were based on 25 mature myxospores for each *Myxobolus* species and are reported in micrometres (µm), with the arithmetic mean and standard deviation followed by the range in parentheses (Lom and Arthur 1989). Line drawings were prepared using CorelDRAW Graphics Suite 2022.

DNA extraction, amplification and sequencing

Myxospores from host bile, preserved in 95% ethanol, were isolated by centrifugation. Total genomic DNA was extracted using a DNeasy Blood and Tissue Kit (Qiagen, Germany), following the manufacturer's instructions for animal tissue. Two sets of myxosporean-specific primers were used: 18E (Hillis and Dixon. 1991) (5'-CTGGTTGATCCTGCCAGT-3') and 18R (Whipps et al. 2003) (5'-CTACGGAAACCTTGTTACG-3') and a second primer pair designed for this study, M1F (5'-TATTAAGCTATAATGCTTAGCCA-3') and M1R (5'-CCCCGTGTTGAGTCGAATTA-3'). Parasite SSU rRNA genes were amplified in 25 µl PCR volumes containing 1 µl of each primer (10 µmol/l), 2 µl genomic DNA, 12.5 µl of 2×Es Taq MasterMix (CWBIO) and 8.5 µl ddH_20, with initial denaturation at 94 °C for 5 min, then 35 cycles of denaturation at 94 °C for 30 s, annealing at 56 °C for 30 s and extension at 72 °C for 2 min, followed by a final extension at 72 °C for 10 min. The PCR products were subjected to electrophoresis on a 1.5% agarose gel. Target bands were excised and purified using a DNA Gel Extraction Kit (Omega Bio-Tek, Norcross, GA, USA). The purified amplicons were ligated into a pMD19-T vector (TaKaRa, Otsu, Japan) and *Escherichia coli* strain DH5a was transformed with this construct. Eight transformants were grown in culture, plasmids purified and four clones were sequenced using an ABI Prism 377 DNA Sequencer. The SSU rDNA sequences of myxospores were assembled using ContigExpress software and were submitted to the National Center for Biotechnology Information (NCBI) nucleotide database for public access.

Molecular and phylogenetic analyses

Sequence similarity and genetic distance were calculated between the newly-obtained SSU rDNA sequence and those showing the highest identity in the NCBI BLAST search, as well as with the morphologically similar species. Pairwise sequence similarity was performed using WATER programme of the EMOSS suite (Madeira et al. 2024) and genetic distances (p-distance) were calculated in MEGA11 (Tamura et al. 2021).

We constructed an alignment of 30 myxosporean SSU rRNA gene sequences, comprising our one new sequence and sequences with similarity over 80% obtained from a BLASTn search of the NCBI database. *Myxidium cuneiforme* (DQ377709) and *Zschokkella nova* (DQ377690) were chosen as outgroup in the SSU rRNA gene phylogenetic tree. Sequence alignment was performed using Clustal X with default settings (Thompson 1997). Subsequently, Gblocks v.0.91b was used to remove highly variable, potentially misaligned or rapidly evolving positions (Castresana 2000), with the following settings: the minimum number of sequences for a conserved position was set to 17, the minimum number of sequences for a flank position was also set to 17, the maximum number of contiguous non-conserved positions was set to 32,000, the minimum length of a block was set to 2 and all gap positions were allowed. Maximum Likelihood (ML) trees were constructed using the RAxML-HPC2 XSEDE (8.2.12) mode available in the online platform, the CIPRES Science Gateway (http://www.phylo.org/), with 1000 bootstrap replicates to assess support values. Bayesian Inference (BI) trees were constructed using MrBayes 3.1.2 (Ronquist and Huelsenbeck 2003), applying the optimal evolutionary model GTR+I+G determined by ModelTest v. 3.7. (Posada and Crandall 1998). The analysis was run for 10,000,000 generations, sampling one tree per 200 generations and discarding the first 25% of samples as burn-in. Consensus trees were generated from the remaining samples. Tree visualisation and editing were performed using FigTree v.1.4.2 and Adobe Photoshop 2022.

Results

Taxonomic summary

Phylum: Cnidaria Hatschek, 1888
Class: Myxozoa Grassé, 1970
Subclass: Myxosporea Bütschli, 1881
Order: Bivalvulida Shulman, 1959
Family: Myxobolidae Thélohan, 1892
Genus: *Myxobolus* Bütschli, 1882

***Myxobolus branchiostegi* sp. nov.**
https://zoobank.org/27053AC2-1CFA-4EC4-89DF-77C372B52C5D

Type host. *Branchiostegus argentatus* Cuvier, 1830 (Perciformes, Malacanthidae).

Type locality. Xiamen (24°41'52"N, 118°10'59"E), East China Sea, China (Fig. 1).

Infection site. Gallbladder.

Date of sampling. 23 July 2017.

Prevalence. Of 28 *B. argentatus* specimens examined, six were infected (21.4%).

Type materials. Syntypes (mounted in glycerine-alcohol-formalin; accession numbers XM2017072306) were deposited in the collection centre of the Animal Biology Key Laboratory of Chongqing Education Commission of China, Chongqing Normal University, Chongqing, China.

Etymology. The specific name *branchiostegi* is derived from the generic name of its host, *Branchiostegus argentatus*.

Description. Vegetative stages were not observed. The mature myxospores are oval in shape, with blunt anterior and posterior ends, in both valvular and sutural views (Fig. 2). Two equal-sized pyriform polar capsules are arranged in an inverted V-shape in the upper half of the myxospore, with their anterior third closely appressed to each other and containing a polar tubule coiled 4–6 turns. The sporoplasm is single and occupies the entire intracapsular cavity beneath the polar capsules, with a small, round nucleus visible in the lower half of the spore. The morphological measurements of mature myxospores (n = 25) are as follows: spore length 9.21 ± 0.52 (8.3–9.8) μm, spore width 7.40 ± 0.60 (6.2–8.0) μm, polar capsule length 4.40 ± 0.34 (3.7–4.8) μm, polar capsule width 2.58 ± 0.17 (2.3–2.9) μm.

Remarks. Morphological comparison with congeners shows that *M. branchiostegi* sp. nov. most closely resembles *Myxobolus arrabonensis* Cech et al. 2015, *Myxobolus cerveirensis* Rocha et al. 2019, *Myxobolus labrosus* Rocha et al. 2019, *Myxobolus squamalis* Iversen, 1954 (Polley et al. 2013) and *Myxobolus urinaris* Rocha et al. 2019 (Table 1). The new species, together with *M. cerveirensis*, *M. squamalis* and *M. urinaris*, possesses ellipsoidal spores with bluntly rounded anterior and posterior

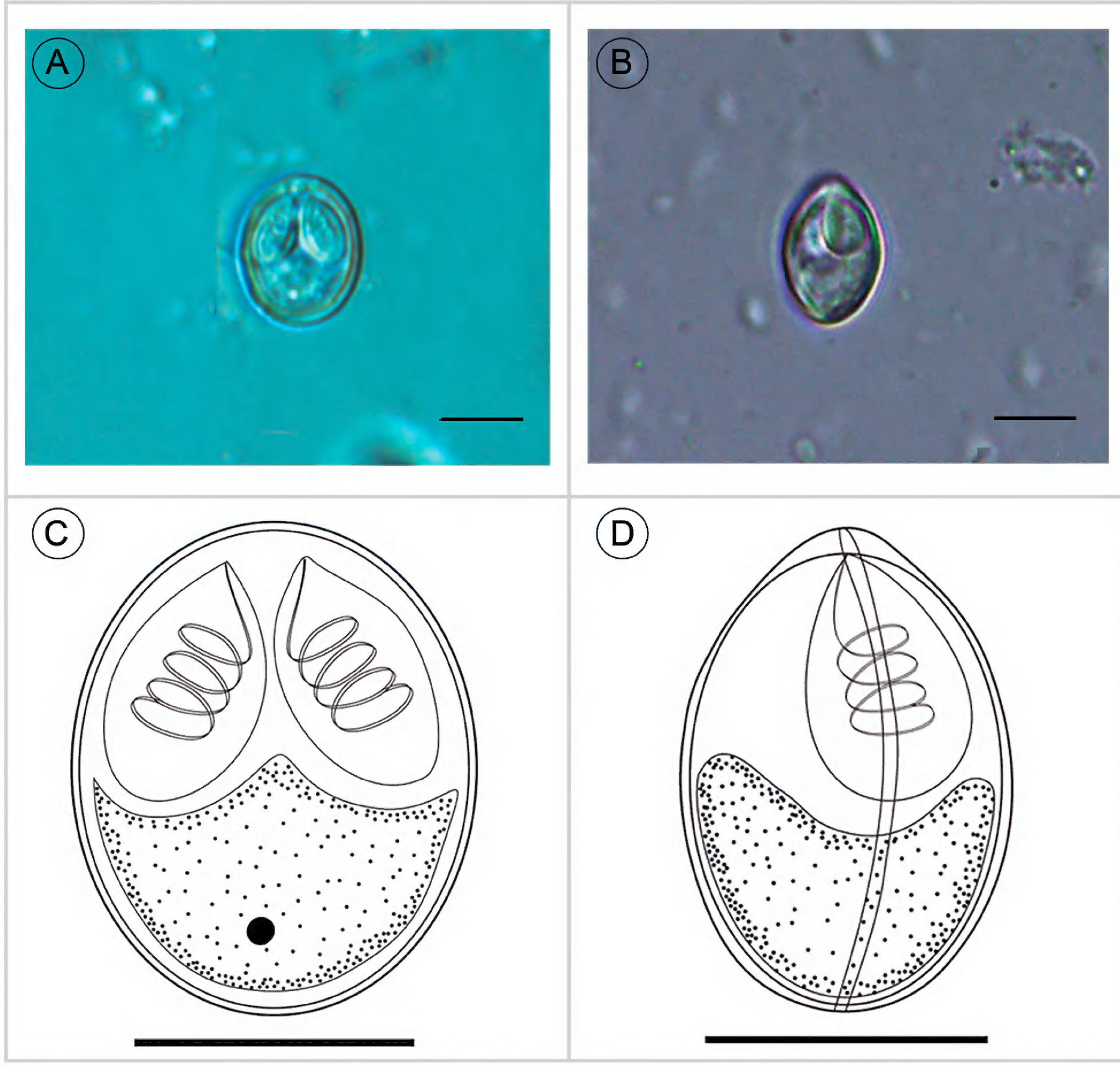

Figure 2. Light micrographs and line drawings of mature myxospores of *Myxobolus branchiostegi* sp. nov. **A.** Valvular view; **B.** Oblique sutural view; **C.** Line drawing of the valvular view; **D.** Line drawing of the oblique sutural view. Scale bars: 5 μm.

Table 1. Comparative morphometrics of *Myxobolus branchiostegi* sp. nov. with the similar species.

Species	Host	SL (µm)	SW (µm)	PCL (µm)	PCW (µm)	NTC	Infection site	Locality	Reference
Myxobolus branchiostegi sp. nov.	*Branchiostegus argentatus* Cuvier, 1830	9.21 ± 0.52 (8.3–9.8)	7.40 ± 0.60 (6.2–8.0)	4.40 ± 0.34 (3.7–4.8)	2.58 ± 0.17 (2.3–2.9)	4–6	Gall bladder	China	This study
Myxobolus arrabonensis Cech et al., 2015	*Chondrostoma nasus* Linnaeus, 1758	8.7 ± 0.6 (8.4–10.0)	7.80 ± 0.34 (7.6–8.0)	4.8 ± 0.44 (4.5–5.9)	2.9 ± 0.12 (2.7–3.1)	4–6	Gill filaments	Hungary	Cech et al. (2015)
Myxobolus cerveirensis Rocha et al., 2019	*Chelon ramada* Risso, 1827	8.1 ± 0.2 (7.7–8.7)	6.8 ± 0.2 (6.7–7.3)	4.2 ± 0.2 (4.0–4.7)	2.8 ± 0.2 (2.3–3.0)	4–5	Intestine	Portugal	Rocha et al. (2019)
Myxobolus labrosus Rocha et al., 2019	*Chelon labrosus* Risso, 1827	10.0 ± 0.2 (9.7–10.3)	8.1 ± 0.3 (7.7–8.7)	4.5 ± 0.2 (4.0–5.0)	2.5 ± 0.2 (2.3–2.7)	5–7	Urinary bladder	Portugal	Rocha et al. (2019)
Myxobolus squamalis Iversen, 1954	*Oncorhynchus mykiss* Walbaum, 1792	9.00 (8.1–9.9)	8.60 (7.7–9.9)	4.40 (3.9–5.1)	3.10 (2.6–3.9)	4	Scales	USA	Polley et al. (2013)
Myxobolus urinaris Rocha et al., 2019	*Mugil cephalus* Linnaeus, 1758	10.0 ± 0.3 (9.3–10.3)	8.2 ± 0.3 (7.7–8.7)	4.0 ± 0.3 (3.3–4.7)	2.8 ± 0.1 (2.7–3.0)	4–5	Urinary bladder	Portugal	Rocha et al. (2019)
Myxobolus iwagiensis Kawano et al., 2025	*Oryzias latipes* Temminck & Schlegel, 1846	12.1 ± 0.4 (11.3–12.8)	9.8 ± 0.3 (9.1–10.5)	6.4 ± 0.2 (5.9–6.9); 5.8 ± 0.3 (5.3–6.5)	4.0 ± 0.2 (3.4–4.4); 3.5 ± 0.2 (3.1–4.0)	6–8; 4–6	Peripheral nerves, beside the gill arch cartilage.	Japan	Kawano et al. (2025)

SL spore length, SW spore width, PCL polar capsule length, PCW polar capsule width, NTC number of coils.

ends in valvular view; however, their dimensions differ subtly. Compared with *M. branchiostegi* sp. nov. (9.21 ± 0.52 µm in length, 7.40 ± 0.60 µm in width), *M. cerveirensis* has slightly shorter and narrower spores (8.1 ± 0.2 µm × 6.8 ± 0.2 µm), *M. squamalis* slightly shorter, but wider spores (9.00 µm × 8.60 µm) and *M. urinaris* slightly longer and wider spores (10.0 ± 0.3 µm × 8.2 ± 0.3 µm). In contrast, *M. arrabonensis* and *M. labrosus* differ more markedly: the former has shorter and wider spores (8.7 ± 0.6 µm × 7.8 ± 0.34 µm), described as "short ellipsoidal" (Cech et al. 2015), while the latter has longer and wider spores (10.0 ± 0.2 µm × 8.1 ± 0.3 µm) with an oval outline (Rocha et al. 2019). Distinct sutural markings are visible in *M. cerveirensis* and *M. labrosus*, whereas they are absent in *M. branchiostegi* sp. nov. Ecologically, the similar species differ in host and infection site: *M. arrabonensis* infects the gill filaments of *Chondrostoma nasus* Linnaeus, 1758; *M. cerveirensis* the intestine of *Chelon ramada* Risso, 1827; *M. labrosus* the urinary bladder of *Chelon labrosus* Risso, 1827; *M. squamalis* the scales of *Oncorhynchus mykiss* Walbaum, 1792; and *M. urinaris* the urinary bladder of *Mugil cephalus* Linnaeus, 1758. In contrast, the new species parasitises the gallbladder of *B. argentatus*. Their geographical ranges are likewise distinct: *M. branchiostegi* sp. nov. is known from China, whereas *M. arrabonensis* occurs in Hungary, *M. cerveirensis*, *M. labrosus* and *M. urinaris* in Portugal and *M. squamalis* in the United States (Table 1).

In addition to the above congeners, *Myxobolus iwagiensis* Kawano et al. 2025, which exhibits the highest sequence similarity (92.0%) to *M. branchiostegi* sp. nov. in the GenBank database, was also included in the morphological comparison. Compared with the present species, *M. iwagiensis* possesses noticeably larger spores in all measured dimensions, including spore length, spore width and the length and width of the polar capsules (Table 1). The two polar capsules in *M. branchiostegi* sp. nov. are equal in size, whereas those of *M. iwagiensis* are unequal. Ecologically, the two species also differ markedly in host and infection site: the new species was discovered in the gallbladder of *B. argentatus* collected from the East China Sea, whereas *M. iwagiensis* was reported from the peripheral nerves and beside the gill-arch cartilage of *Oryzias latipes* Temminck & Schlegel, 1846, the species being obtained from a brackish reservoir in Japan.

Molecular analyses

A partial SSU rDNA sequence of *M. branchiostegi* sp. nov. (1848 bp) was deposited in GenBank under the accession number PV866587. BLASTn search revealed that SSU rDNA sequence of *M. branchiostegi* sp. nov. was unique amongst all myxozoans in GenBank. The molecular analysis revealed that this sequence exhibited the highest similarity (92.0%) and the shortest genetic distance (0.0653) to *M. iwagiensis* (GenBank: LC861743). The SSU rDNA sequences of all species, except *M. iwagiensis*, showed less than 80% similarity and genetic distances greater than 0.3 relative to the novel species (Table 2).

Phylogenetic analyses

Phylogenetic trees constructed, based on SSU rDNA sequences using Maximum-Likelihood (ML) and Bayesian-Inference (BI) methods, exhibited consistent topologies (Fig. 3). *Nephrocystidium pickii* Weissenberg, 1921 occupied the basal position of the phylogenetic tree, whereas the remaining taxa formed two well-supported (PP = 1.00, BS = 100) monophyletic lineages: the Ortholineidae lineage and the Myxobolidae lineage (Fig. 3). Within the Myxobolidae lineage, two major clades were recovered: Clade A and Clade B. In Clade A, *Myxobolus acinosus* Nie & Li, 1973 diverged first, forming a distinct basal subclade, whereas all freshwater *Henneguya* species, together with several freshwater *Myxobolus* species, grouped into another subclade (Fig. 3, Clade A). Clade B comprised three subclades. Subclade I contained the novel marine species *M. branchiostegi* sp. nov. and the brackish-water *M. iwagiensis*, which were recovered as sister taxa. Subclade II consisted of the brackish-water species

Table 2. SSU rDNA sequence similarity (upper triangle) and genetic distance (lower triangle) amongst *Myxobolus branchiostegi* sp. nov. and related *Myxobolus* species.

Species	1	2	3	4	5	6	7	8	9	10
1- *Myxobolus branchiostegi* sp. nov. (PV866587)		92.0%	69.8%	70.8%	71.0%	68.6%	68.3%	69.0%	69.9%	68.1%
2- *Myxobolus iwagiensis* (LC861743)	0.0653		71.7%	70.1%	70.7%	68.8%	68.3%	70.5%	69.8%	68.5%
3- *Myxobolus* cf. *colossomatis* (KF597017)	0.3355	0.3342		83.7%	82.8%	72.0%	73.4%	72.9%	73.3%	71.9%
4- *Myxobolus colossomatis* (MK032220)	0.3319	0.3271	0.0997		80.4%	73.4%	71.4%	71.5%	73.3%	72.5%
5- *Myxobolus batalhensis* (MF361091)	0.3476	0.3303	0.1460	0.1518		73.4%	72.1%	72.8%	72.2%	69.6%
6- *Myxobolus arrabonensis* (MH375073)	0.3712	0.3803	0.2557	0.2688	0.2685		74.1%	73.4%	76.0%	75.0%
7- *Myxobolus cerveirensis* (MK203079)	0.3719	0.3719	0.2742	0.2715	0.2669	0.2705		88.7%	74.6%	84.0%
8- *Myxobolus labrosus* (MK203081)	0.3380	0.3369	0.2588	0.2673	0.2660	0.2492	0.0952		74.9%	84.9%
9- *Myxobolus squamalis* (JX910363)	0.3001	0.3076	0.2497	0.2374	0.2367	0.2193	0.2362	0.2118		73.6%
10- *Myxobolus urinaris* (MK203083)	0.3614	0.3582	0.2883	0.2951	0.2796	0.2751	0.1192	0.1185	0.2333	

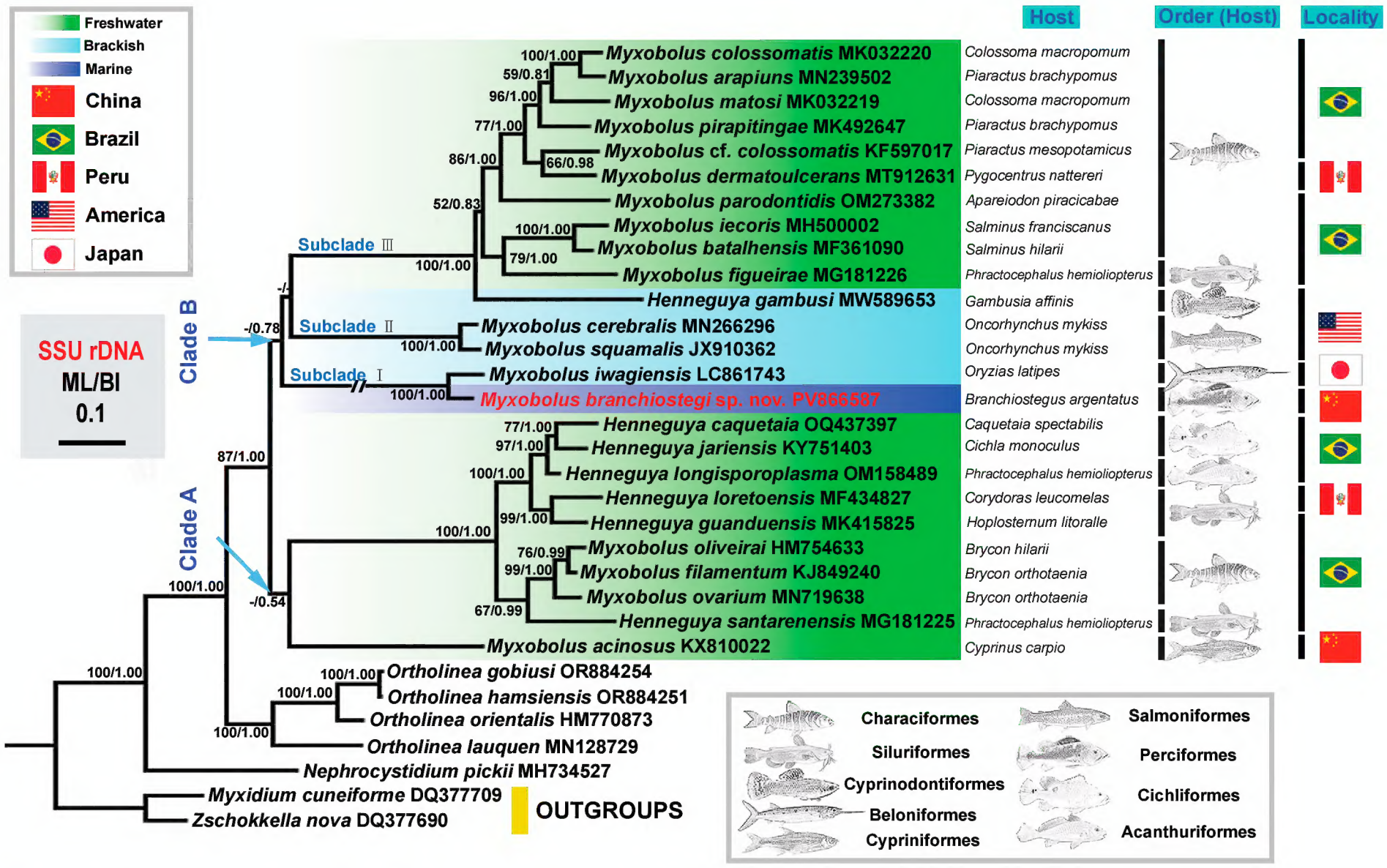

Figure 3. Bayesian Inference (BI) and Maximum Likelihood (ML) phylogenetic tree, based on SSU rRNA gene sequences of *Myxobolus branchiostegi* sp. nov. and closely-related species. Numbers at the nodes indicate Bayesian posterior probabilities and ML bootstrap support; "-" denotes support values below 50%. "//" indicates that the branch is shown at one-third of its original length.

Myxobolus cerebralis Hofer, 1903 and *M. squamalis*, also forming a sister-taxa relationship. Subclade III included the majority of freshwater *Myxobolus* species together with the brackish-water *Henneguya gambusi* Parker et al., 1971, the latter occupying a basal position within this subclade. Subclade II and Subclade III were recovered as sister groups, together forming a lineage sister to Subclade I (Fig. 3, Clade B).

Overall, the phylogenetic results support the monophyly of the family Myxobolidae; however, neither the genus *Myxobolus* nor *Henneguya* was resolved as monophyletic.

Discussion

In the present study, we describe a novel *Myxobolus* species infecting the gallbladder of *B. argentatus* from the coastal waters of Xiamen, Fujian Province, China. Hitherto, this is the first report of *Myxobolus* species parasitising *B. argentatus*. Though there is no specified benchmark for inter-species SSU rRNA gene variation, values of 1.0–1.3% are suggestive of different taxa supported by other characters such as host, infection site or morphometry (Gunter and Adlard 2009; Gunter et al. 2009; Heiniger and Adlard 2013). In this study, the new species exhibited an 8.00% sequence variation from its closest known relative, *M. iwagiensis*, which far exceeds the accepted threshold for species delineation. Taken together with the distinct morphological differences from the most morphologically similar species, as described in the "Remarks" section, these findings strongly support its designation as a novel species.

Previous studies have shown that phylogenetically related myxosporeans tend to infect closely-related fish hosts, typically within the same order (Zago et al. 2022; Zhang et al. 2023; Velasco et al. 2024; de Sena et al. 2025). Consistent with this, the phylogenetic analysis in the present study revealed that the many Myxobolidae species cluster according to the taxonomic affiliation of their hosts, with closely-related parasites infecting hosts within the same order (Fig. 3). For instance, within Clade A, *Henneguya jariensis* Zatti et al., 2018 and *Henneguya caquetaia* Figueredo et al., 2023, both parasitising Cichliformes fishes, form a distinct cluster, while *Myxobolus oliveirai* Milanin et al., 2010, *Myxobolus filamentum* Naldoni et al., 2015 and *Myxobolus ovarium* Naldoni et al., 2020, all infecting Characiformes hosts, also group together. In Clade B, *M. cerebralis* and *M. squamalis*, both parasites of Salmoniformes fishes, are closely associated. Moreover, within Subclade III, with the exception of *Myxobolus figueirae* Naldoni et al., 2018 and *H. gambusi*, all taxa infect Characiformes hosts.

However, some host orders are shared by parasites from multiple, phylogenetically distant lineages. For instance, *Henneguya loretoensis* Mathews et al., 2017, *Henneguya guanduensis* Abdallah et al., 2007 and *Henneguya santarenensis* Naldoni et al., 2018, all infecting Siluriformes fishes, occur in different sublineages within Clade A: *H. loretoensis* and *H. guanduensis* form a single cluster,

whereas *H. santarenensis* occupies a separate, distantly related branch. Similarly, *M. figueirae*, which also parasitises siluriform hosts, is placed in Clade B (Fig. 3). The causes underlying deviations from the general pattern described above are likely multifactorial. One plausible explanation is that some parasites may expand their host range or acquire new hosts through host-switching events (Holzer et al. 2018). Such processes could account for the occurrence of lineages in which most species infect hosts from a single order, but a few members parasitize hosts from different orders (Forró and Eszterbauer 2016; Elloumi et al. 2023; Rocha et al. 2023). For example, within the freshwater lineage of Subclade III, all taxa, except *M. figueirae*, infect Characiformes fishes. This suggests that the ancestral host of *M. figueirae* was likely a characiform, with its current siluriform host representing a more recent acquisition via host-switching or host-range expansion (Naldoni et al. 2018).

The phylogenetic analysis revealed a pronounced clustering of myxobolid species according to their aquatic habitat, with distinct and well-supported clades corresponding to marine, freshwater and brackish-water hosts, a pattern consistent with previous reports (Fiala et al. 2015; Holzer et al. 2018). For instance, all freshwater *Henneguya* species, together with several freshwater *Myxobolus* species, form a well-supported assemblage within Clade A (Fig. 3). The novel species *M. branchiostegi* sp. nov., infecting a marine fish host, clusters with the brackish-water species *M. iwagiensis*, constituting Subclade I of Clade B. This subclade is recovered as the sister group to a lineage comprising Subclade II (exclusively brackish-water species) and Subclade III (species from both brackish-water and freshwater habitats) within Clade B (Fig. 3).

Based on the phylogenetic patterns observed in Clade B, it is plausible that the evolutionary history of *Myxobolus* species involved a habitat shift from marine to brackish-water and, subsequently, to freshwater environments, potentially facilitated by historical marine transgressions (Zatti et al. 2017). Consistent with this scenario, previous studies have documented an increasing number of cases in which parasites formerly restricted to marine or brackish-water habitats are now reported infecting freshwater fishes in South America (Zatti et al. 2018, 2020; Alama-Bermejo et al. 2021; Franzolin et al. 2022). However, as noted by Fiala and Bartošová (2010), species of the genus *Myxobolus* are predominantly parasites of freshwater fishes. Although the ancestral myxosporeans were marine, the progenitor of *Myxobolus* is hypothesised to have been a freshwater species. The observed phylogenetic patterns suggest that habitat transitions may have played a role in the diversification of *Myxobolus* species; however, this hypothesis requires further testing. Integrating additional molecular data with detailed ecological and host information from extant taxa will be essential to better understand the evolutionary pathways and potential habitat shifts within the genus.

The phylogenetic analyses also indicate a potential link between the geographic distribution of myxosporean species and their phylogenetic relationships. This tendency was observed in earlier studies (Rocha et al. 2023; Velasco et al. 2024), although it was not considered predominant. This relationship is exemplified by the novel species *M. branchiostegi* sp. nov., collected from the East China Sea, which clusters as sister to the Japanese species *M. iwagiensis*. Given the hydrological connectivity between the East China Sea and the Sea of Japan, these contiguous marine regions may serve as continuous habitats or dispersal corridors, thereby maintaining close evolutionary relationships between their parasite fauna. Furthermore, all Brazilian myxosporeans assigned to Clade B form a well-supported lineage together with *Myxobolus dermatoulcerans* Stilwell et al. 2020 from Peru and Brazilian representatives of Clade A cluster with *H. loretoensis*, also from Peru (Fig. 3). Considering that Brazil and Peru are geographically adjacent and share interconnected freshwater systems within the Amazon Basin (Medeiros et al. 2015), which is the largest drainage basin in the world, it is plausible that myxosporean taxa from these regions originated from a common ancestral lineage. Collectively, these results highlight the potential role of geographic proximity and drainage basin connectivity in shaping the phylogeographic structure of this parasite group.

In summary, we provide robust taxonomic evidence for the establishment of *M. branchiostegi* sp. nov. through an integrative approach encompassing detailed morphological characterisation, molecular analyses and infection characteristics.

Statements and declarations

Funding

This work was supported by grants from the National Natural Science Foundation of China (No. 31970409), the Chongqing Natural Science Foundation of China (No. CSTB2022NSCQ-MSX0994) and the Science and Technology Research Key Program of Chongqing Municipal Education Commission (No. KJZD-K202300503).

Author contributions

Conceptualisation: Chengzhong Yang and Yuanjun Zhao. Formal analysis: Chengzhong Yang, Yalin Xiong and Mao Wang. Funding acquisition: Chengzhong Yang and Yuanjun Zhao. Supervision: Chengzhong Yang. Writing–original draft: Chengzhong Yang, Yalin Xiong, Xue Chen. Writing–review and editing: Yalin Xiong, Xue Chen, Jianjun Peng, Xiaojuan Cui and Chengzhong Yang.

Competing interests

The authors declare no competing interests.

Data availability

The small subunit ribosomal RNA (SSU rRNA) gene sequence generated in this study has been deposited in GenBank under the accession number PV866587. All of the data that support the findings of this study are available in the main text.

References

Alama-Bermejo G, Hernández-Orts JS, Huchon D, Atkinson SD (2021) Two novel myxosporean parasite species of *Ceratomyxa* Thélohan, 1892 from the banded cusk-eel *Raneya brasiliensis* (Kaup) (Ophidiiformes: Ophidiidae) off Patagonia, Argentina. Parasitology International 85: 102433. https://doi.org/10.1016/j.parint.2021.102433

Alexander JD, Hallett SL, Stocking RW, Xue L, Bartholomew JL (2014) Host and parasite populations after a ten year flood: *Manayunkia speciosa* and *Ceratonova* (syn *Ceratomyxa*) *shasta* in the Klamath River. Northwest Science 88(3): 219–233. https://doi.org/10.3955/046.088.0305

Boreham RE, Hendrick S, O'donoghue PJ, Stenzel DJ (1998) Incidental finding of *Myxobolus* spores (Protozoa: Myxozoa) in stool samples from patients with gastrointestinal symptoms. Journal of Clinical Microbiology 36(12): 3728–3730. https://doi.org/10.1128/jcm.36.12.3728-3730.1998

Carraro L, Mari L, Hartikainen H, Strepparava N, Wahli T, Jokela J, Gatto M, Rinaldo A, Bertuzzo E (2016) An epidemiological model for proliferative kidney disease in salmonid populations. Parasites & Vectors 9(1): 487. https://doi.org/10.1186/s13071-016-1759-z

Castresana J (2000) Selection of conserved blocks from multiple alignments for their use in phylogenetic analysis. Molecular Biology and Evolution 17(4): 540–552. https://doi.org/10.1093/oxfordjournals.molbev.a026334

Cech G, Borzák R, Molnár K, Székely C (2015) Three new species of *Myxobolus* Bütschli, 1882 (Myxozoa: Myxobolidae) infecting the common nase *Chondrostoma nasus* (L.) in the River Danube. Systematic Parasitology 92(2): 101–111. https://doi.org/10.1007/s11230-015-9589-5

de Sena NM, Eduard J, Pereira CMB, Neto JLS, Velasco M (2025) *Myxobolus medusae* n. sp., a new species of Myxozoa with dendritic appendages. Parasitology International 103106. https://doi.org/10.1016/j.parint.2025.103106

Eiras JC, Molnár K, Lu Y (2005) Synopsis of the species of *Myxobolus* Bütschli, 1882 (Myxozoa: Myxosporea: Myxobolidae). Systematic Parasitology 61(1): 1–46. https://doi.org/10.1007/s11230-004-6343-9

Eiras JC, Zhang J, Molnár K (2014) Synopsis of the species of *Myxobolus* Bütschli, 1882 (Myxozoa: Myxosporea, Myxobolidae) described between 2005 and 2013. Systematic Parasitology 88(1): 11–36. https://doi.org/10.1007/s11230-014-9484-5

Eiras JC, Cruz CF, Saraiva A, Adriano EA (2021) Synopsis of the species of *Myxobolus* (Cnidaria, Myxozoa, Myxosporea) described between 2014 and 2020. Folia Parasitologica 68: 012. http://doi.org/10.14411/fp.2021.012

Elloumi A, Rangel LF, Santos MJ, Bahri S (2023) *Myxidium tunisiensis* n. sp. (Myxosporea: Myxidiidae) infecting the rough skate *Raja radula* Delaroche, 1908 (Rajiformes: Rajidae) from North East Tunisia. Parasitology Research 122(1): 19–33. https://doi.org/10.1007/s00436-021-07306-5

Fiala I, Bartošová P (2010) History of myxozoan character evolution on the basis of rDNA and EF-2 data. BMC Evolutionary Biology 10: 228. https://doi.org/10.1186/1471-2148-10-228

Fiala I, Bartošová-Sojková P, Whipps CM (2015) Classification and phylogenetics of Myxozoa. In: Okamura B, Gruhl A, Bartholomew JL (Eds) Myxozoan evolution, ecology and development. Springer International Publishing, Cham, 85–110. https://doi.org/10.1007/978-3-319-14753-6_5

Forró B, Eszterbauer E (2016) Correlation between host specificity and genetic diversity for the muscle-dwelling fish parasite *Myxobolus pseudodispar*: Examples of myxozoan host-shift? Folia Parasitologica 63: 1. https://doi.org/10.14411/fp.2016.019

Franzolin GN, Araújo B, Zatti SA, Naldoni J, Adriano EA (2022) Occurrence of the host-parasite system *Raphiodon vulpinus* and *Ceratomyxa barbata* n. sp. in the two largest watersheds in South America. Parasitology International 91: 102651. https://doi.org/10.1016/j.parint.2022.102651

Gao L, Zhang J, Yang CZ, Zhao YJ (2020) *Myxobolus jialingensis* n. sp. (Myxozoa: Myxobolidae) infecting urinary bladder and hepatopancreas of yellowhead catfish *Tachysurus fulvidraco* from China. Zootaxa 4819(1): 179–186. https://doi.org/10.11646/zootaxa.4819.1.10

Gunter NL, Adlard RD (2009) Seven new species of *Ceratomyxa* Thélohan, 1892 (Myxozoa) from the gall-bladders of serranid fishes from the Great Barrier Reef, Australia. Systematic Parasitology 73(1): 1–11. https://doi.org/10.1007/s11230-008-9162-6

Gunter NL, Whipps CM, Adlard RD (2009) *Ceratomyxa* (Myxozoa: Bivalvulida): robust taxon or genus of convenience? International Journal for Parasitology 39(12): 1395–1405. https://doi.org/10.1016/j.ijpara.2009.04.008

Guo R, Zhang SP, Jiang XB, Wang W, Wang HC, Cai LM, Yang XQ (2021) Molecular identification and phylogenetic analysis of *Myxobolus honghuensis* found in pharynx of goldfish *Carassius auratus.* Journal of Fisheries Research 43(1): 61–66.

Harada T, Kawai T, Jinnai M, Ohnishi T, Sugita-Konishi Y, Kumeda Y (2012) Detection of *Kudoa septempunctata* 18S ribosomal DNA in patient fecal samples from novel food-borne outbreaks caused by consumption of raw olive flounder (*Paralichthys olivaceus*). Journal of Clinical Microbiology 50(9): 2964–2968. https://doi.org/10.1128/jcm.01218-12

Heiniger H, Adlard R (2013) Molecular identification of cryptic species of *Ceratomyxa* Thélohan, 1892 (Myxosporea: Bivalvulida) including the description of eight novel species from apogonid fishes (Perciformes: Apogonidae) from Australian waters. Acta Parasitologica 58(3): 342–360. https://doi.org/10.2478/s11686-013-0149-3

Hillis DM, Dixon MT (1991) Ribosomal DNA: Molecular evolution and phylogenetic inference. The Quarterly Review of Biology 66(4): 411–453. https://doi.org/10.1086/417338

Holzer AS, Bartošová-Sojková P, Born-Torrijos A, Lövy A, Hartigan A, Fiala I (2018) The joint evolution of the Myxozoa and their alternate hosts: A cnidarian recipe for success and vast biodiversity. Molecular Ecology 27(7): 1651–1666. https://doi.org/10.1111/mec.14558

Kawano KM, Sakurai M, Yanagida T (2025) Description of *Myxobolus iwagiensis* n. sp. (Myxosporea: Myxobolidae), infecting medaka *Oryzias latipes* (Temminck & Schlegel, 1846) (Beloniformes: Adrianichthyidae) in Japan. Parasitology International 108: 103074. https://doi.org/10.1016/j.parint.2025.103074

Kim JJ, Ryu S, Lee H (2018) Foodborne illness outbreaks in Gyeonggi province, Korea, following seafood consumption potentially

caused by *Kudoa septempunctata* between 2015 and 2016. Osong Public Health and Research Perspectives 9(2): 66. https://doi.org/10.24171/j.phrp.2018.9.2.05

Liu XC, Yang CZ, Zhao YJ (2016) Redescription of *Myxobolus honghuensis* Liu et al. 2012 and identification on its genetic related species. Acta Hydrobiologica Sinica 40(2): 350–357.

Liu XH, Zhang DD, Yang CZ, Zhao YJ (2019) Morphological and molecular identification of *Myxobolus parakoi* sp. nov. (Myxozoa: Myxobolidae), from *Cyprinus carpio* in Chongqing China. Zootaxa 4657(1): 117–126. https://doi.org/10.11646/zootaxa.4657.1.4

Lom J, Arthur JR (1989) A guideline for the preparation of species descriptions in Myxosporea. Journal of Fish Diseases 12: 151–156. https://doi.org/10.1111/j.1365-2761.1989.tb00287.x

Lom J, Dyková I (2006) Myxozoan genera: Definition and notes on taxonomy, life-cycle terminology and pathogenic species. Folia Parasitologica 53: 1–36. https://doi.org/10.14411/fp.2006.001

Madeira F, Madhusoodanan N, Lee J, Eusebi A, Niewielska A, Tivey ARN, Lopez R, Butcher S (2024) The EMBL-EBI Job Dispatcher sequence analysis tools framework in 2024. Nucleic Acids Research 52(W1): W521–W525. https://doi.org/10.1093/nar/gkae241

Medeiros PM, Seidel M, Ward ND, Carpenter EJ, Gomes HR, Niggemann J, Krusche AV, Richey JE, Yager PL, Dittmar T (2015) Fate of the Amazon River dissolved organic matter in the tropical Atlantic Ocean. Global Biogeochemical Cycles 29(5): 677–690. https://doi.org/10.1002/2015GB005115

Naldoni J, Maia AA, Correa LL, da Silva MR, Adriano EA (2018) New myxosporeans parasitizing *Phractocephalus hemioliopterus* from Brazil: Morphology, ultrastructure and SSU-rDNA sequencing. Diseases of Aquatic Organisms 128(1): 37–49. https://doi.org/10.3354/dao03210

Okamura B, Gruhl A, Bartholomew JL (2015) An introduction to myxozoan evolution, ecology and development. In: Okamura B, Gruhl A, Bartholomew JL (Eds) Myxozoan evolution, ecology and development. Springer International Publishing, Cham, 1–20. https://doi.org/10.1007/978-3-319-14753-6_1

Okamura B, Hartigan A, Naldoni J (2018) Extensive uncharted biodiversity: The parasite dimension. Integrative and Comparative Biology 58(6): 1132–1145. https://doi.org/10.1093/icb/icy039

Polley TM, Atkinson SD, Jones GR, Bartholomew JL (2013) Supplemental description of *Myxobolus squamalis* (Myxozoa). The Journal of Parasitology 99(4): 725–728. https://doi.org/10.1645/12-109.1

Posada D, Crandall KA (1998) MODELTEST: Testing the model of DNA substitution. Bioinformatics (Oxford, England) 14(9): 817–818. https://doi.org/10.1093/bioinformatics/14.9.817

Rocha S, Casal G, Alves Â, Antunes C, Rodrigues P, Azevedo C (2019) Myxozoan biodiversity in mullets (Teleostei, Mugilidae) unravels hyperdiversification of *Myxobolus* (Cnidaria, Myxosporea). Parasitology Research 118(12): 3279–3305. https://doi.org/10.1007/s00436-019-06476-7

Rocha S, Filipe Rangel L, Casal G, Severino R, Soares F, Rodrigues P, Santos MJ (2023) Occurrence of two myxosporean parasites in the gall bladder of white seabream *Diplodus sargus* (L.) (Teleostei, Sparidae), with the morphological and molecular description of *Ceratomyxa sargus* n. sp. PeerJ 11: e14599. https://doi.org/10.7717/peerj.14599

Ronquist F, Huelsenbeck JP (2003) MrBayes 3: Bayesian phylogenetic inference under mixed models. Bioinformatics (Oxford, England) 19(12): 1572–1574. https://doi.org/10.1093/bioinformatics/btg180

Saha M, Bandyopadhyay PK (2018) Identification of a new myxosporean parasite *Thelohanellus indiana* n. sp. (Myxosporea: Myxobolidae) isolated from three major organs of goldfish, *Carassius auratus* L. highlighted with its morphological and SSU rDNA sequence based molecular description. Microbial Pathogenesis 122: 191–199. https://doi.org/10.1016/j.micpath.2018.05.038

Shi XW, Wang M, Chen HZ, Gao L, Liu XC, Yang CZ, Zhao YJ (2022) Redescription and molecular phylogenetic analysis on *Myxobolus acutus* Wu & Chen, 1987 (Myxozoa: Myxobolidae). Acta Hydrobiologica Sinica 46(4): 389–396. https://doi.org/10.7541/2021.2021.0267

Székely C, Cech G, Atkinson SD, Molnár K, Egyed L, Gubányi A (2015) A novel myxozoan parasite of terrestrial mammals: Description of *Soricimyxum minuti* sp. n. (Myxosporea) in pygmy shrew *Sorex minutus* from Hungary. Folia Parasitologica 62. https://doi.org/10.14411/fp.2015.045

Tamura K, Stecher G, Kumar S (2021) MEGA11: Molecular Evolutionary Genetics Analysis version 11. Molecular Biology and Evolution 38: 3022–3027. https://doi.org/10.1093/molbev/msab120

Thompson JD (1997) The CLUSTAL_X windows interface: Flexible strategies for multiple sequence alignment aided by quality analysis tools. Nucleic Acids Research 25(24): 4876–4882. https://doi.org/10.1093/nar/25.24.4876

Tilley MF, Barry D, Hanington PC, Goater CP (2024) Description, life cycle, and development of the myxozoan *Myxobolus rasmusseni* n. sp. in fathead minnows, *Pimephales promelas*: A possible emerging pathogen in southern Alberta, Canada. International Journal for Parasitology. Parasites and Wildlife 24: 100944. https://doi.org/10.1016/j.ijppaw.2024.100944

Velasco M, Eduard J, Lago IBA, Netto WBG, Dias LDNS, Sindeaux-Neto JL (2024) Histopathological and phylogenetic description of an Amazonian cnidaria microparasite *Myxobolus rousseauxii* n. sp. infecting the gill arches of *Brachyplatystoma rousseauxii* (Siluriformes). Parasitology International 103: 102943. https://doi.org/10.1016/j.parint.2024.102943

Vieira DHMD, Osaki-Pereira MM, Abdallah VD, Oliveira SLP, Duarte AGT, da Silva RJ, de Azevedo RK (2024) Morphological and molecular analysis describing two new species of *Myxobolus* (Cnidaria, Myxosporea) in *Mugil curema* (Mugilidae) from Brazil. Taxonomy 4(3): 548–560. https://doi.org/10.3390/taxonomy4030026

Whipps CM, Adlard RD, Bryant MS, Lester RJ, Findlav V, Kent ML (2003) First report of three *Kudoa* species from eastern Australia: *Kudoa thyrsites* from mahi mahi (*Coryphaena hippurus*), *Kudoa amamiensis* and *Kudoa minithyrsites* n. sp. from sweeper (*Pempheris ypsilychnus*). The Journal of Eukaryotic Microbiology 50(3): 215–219. https://doi.org/10.1111/j.1550-7408.2003.tb00120.x

Yang CZ, Zhou Y, Zhao YJ, Huang W, Huang C (2017) Erection of *Unicapsulocaudum mugilum* gen. et sp. nov. (Myxozoa: Ceratomyxidae) based on its morphological and molecular data. Journal of Natural History 51(9–10): 457–467. https://doi.org/10.1080/00222933.2017.1303096

Yang CZ, Huang Y, Atkinson SD, Bartholomew JL, Ma HG, Zhao YJ (2023) Morphological and genetic analysis of *Ceratomyxa saurida* Zhao et al. 2015 and *Ceratomyxa mai* sp. nov. (Myxozoa: Ceratomyxidae) from the East China Sea. International Journal of Systematic and Evolutionary Microbiology 73(1): 005662. https://doi.org/10.1099/ijsem.0.005662

Zago AC, Vieira DHMD, Franceschini L, da Silva RJ (2022) Morphological, ultrastructural, and molecular analysis of a new species of *Myxobolus* (Cnidaria, Myxosporea) parasitizing *Apareiodon piracicabae* (Characiformes, Parodontidae) from Brazil. Parasitology International 88: 102556. https://doi.org/10.1016/j.parint.2022.102556

Zatti SA, Atkinson SD, Bartholomew JL, Maia AAM, Adriano EA (2017) Amazonian waters harbour an ancient freshwater *Ceratomyxa* lineage (Cnidaria: Myxosporea). Acta Tropica 169: 100–106. https://doi.org/10.1016/j.actatropica.2017.02.006

Zatti SA, Atkinson SD, Maia AMM, Corrêa LL, Bartholomew JL, Adriano EA (2018) Novel *Myxobolus* and *Ellipsomyxa* species (Cnidaria: Myxozoa) parasitizing *Brachyplatystoma rousseauxii* (Siluriformes: Pimelodidae) in the Amazon basin, Brazil. Parasitology International 67: 612–621. https://doi.org/10.1016/j.parint.2018.06.005

Zatti SA, Maia AAM, Adriano EA (2020) Growing diversity supports radiation of an *Ellipsomyxa* lineage into the Amazon freshwater: Description of two novel species parasitizing fish from Tapajós and Amazon rivers. Acta Tropica 211: 105616. https://doi.org/10.1016/j.actatropica.2020.105616

Zhang DD, Zhao YJ, Yang SH, Yang CZ (2019) Morphological and molecular identification of a novel species, *Ceratomyxa siganicola* n. sp. (Myxozoa: Ceratomyxidae) from *Siganus fuscescens*, in East China sea. Acta Parasitologica 64(3): 596–602. https://doi.org/10.2478/s11686-019-00077-1

Zhang B, Tu X, Gu Z (2023) *Myxobolus shuifuensis* sp. n. (Myxozoa: Myxobolidae) infecting the exotic mrigal *Cirrhinus mrigala* feral in China. Parasitology International 94: 102732. https://doi.org/10.1016/j.parint.2023.102732

Zhao YJ, Ma CL, Song WB (2001) Illustrated guide to the identification of pathogenetic protozoa in mariculture – II Diagnostic methods for the myxosporean. Journal of the Ocean University of Qingdao 31: 681–688.

Zhao YJ, Li NN, Tang FH, Dong J (2013) Remarks on the validity of *Myxobolus ampullicapsulatus* and *Myxobolus honghuensis* (Myxozoa: Myxosporea) based on SSU rDNA sequences. Parasitology Research 112(11): 3817–3823. https://doi.org/10.1007/s00436-013-3569-y